Title

Towards a nanoparticle-based prophylactic for maternal autoantibody-related autism

Authors

Bolandparvaz, Amir
Harriman, Rian
Alvarez, Kenneth
et al.

Publication Date

2019-10-01

DOI

10.1016/j.nano.2019.102067

Peer reviewed

HHS Public Access

Author manuscript

Nanomedicine. Author manuscript; available in PMC 2020 May 04.

Published in final edited form as:

Nanomedicine. 2019 October ; 21: 102067. doi:10.1016/j.nano.2019.102067.

Towards a nanoparticle-based prophylactic for maternal autoantibody-related autism

Amir Bolandparvaz, BS[a], **Rian Harriman, BS**[a], **Kenneth Alvarez, BS**[a], **Kristina Lilova, PhD**[b], **Zexi Zang, BS**[a], **Andy Lam, BS**[b], **Elizabeth Edmiston, PhD**[c], **Alexandra Navrotsky, PhD**[b], **Natalia Vapniarsky, PhD**[d], **Judy Van de Water, PhD**[c,e], **Jamal S. Lewis, PhD**[a]

[a]University of California, Davis, Department of Biomedical Engineering, Davis, CA, USA

[b]University of California, Davis, Peter A. Rock Thermochemistry Laboratory and NEAT, Davis, CA, USA

[c]University of California, Davis, Department of Internal Medicine, Division of Rheumatology, Allergy, and Clinical Immunology, Davis, CA, USA

[d]University of California, Davis, Department of Pathology Microbiology and Immunology, Davis, CA, USA

[e]University of California, Davis, M.I.N.D. (Medical Investigation of Neurodevelopmental Disorders), Davis, CA, USA

Abstract

Recently, the causative agents of Maternal Autoantibody-Related (MAR) autism, pathological autoantibodies and their epitopic targets (e.g. lactate dehydrogenase B [LDH B] peptide), have been identified. Herein, we report on the development of Systems for Nanoparticle-based Autoantibody Reception and Entrapment (SNAREs), which we hypothesized could scavenge disease-propagating MAR autoantibodies from the maternal blood. To demonstrate this functionality, we synthesized 15 nm dextran iron oxide nanoparticles surface-modified with citric acid, methoxy PEG(10 kDa) amine, and LDH B peptide (33.8 μg peptide/cm2). In vitro, we demonstrated significantly lower macrophage uptake for SNAREs compared to control NPs. The hallmark result of this study was the efficacy of the SNAREs to remove 90% of LDH B autoantibody from patient-derived serum. Further, in vitro cytotoxicity testing and a maximal tolerated dose study in mice demonstrated the safety of the SNARE formulation. This work establishes the feasibility of SNAREs as the first-ever prophylactic against MAR autism.

Graphical abstract

Author contribution

A.B. contributed to the design and execution of experiments, analysis of data and compilation of the manuscript. K.A., K.L., Z.Z., A.L., and N.V. contributed to the execution of experiments and analysis of data. A.N., E.E., and J.V. collaborated and guided experimental design. J.S.L contributed to the design of experiments, analysis of data, and manuscript compilation. J.S.L has primary responsibility for the content of the manuscript.

Appendix A. Supplementary data

The following are the supplementary data related to this article.

Conflict of Interest: Dr. Van de Water has a patent application involving the MAR ASD peptides described herein; all other authors have no conflicts of interest to declare.

Nanoparticle prophylactic against MAR Autism: **(A)** Autoantigen-coated Dextran Iron Oxide Nanoparticles (DIONPs) formulation are inject intravenously (I.V.). **(B)** Autoantigen-conjugated DIONPs will ligate MAR auto-Abs in the mother's blood. **(C)** Clearance of pathological autoantibodies by liver and phagocytes resulting in normal fetal development.

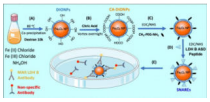

Keywords

Maternal autoantibody-related autism$_1$; Iron oxide$_2$; nanoparticles$_3$; Peptide-functionalized$_4$

Introduction

Autism was first described by Leo Kanner, an American psychiatrist, in 1943 as a neurodevelopmental disorder characterized by impaired communication and repetitive stereotypical behaviors.[1] Since then, autism has been given a broader classification as autism spectrum disorder (ASD), comprised of a wide range of symptoms, skills, and stages of disability. In the United States, 1 in 59 children is born with ASD which amounts to an estimated $268 billion in annual economic burden.2., 3. Currently, there are only post-symptomatic behavioral and pharmacological interventions for ASD treatment. Behavioral mediations to mitigate symptoms of autism include verbal and cognitive behavioral therapy, while off-label drugs generally used for attention deficit hyperactivity disorder (ADHD) (*e.g.* Adderall or Ritalin), depression, and sleep disturbances are the "pharmacological" gold standard.[4] Although the root cause of ASD is yet to be fully elucidated, a combination of genetic and environmental factors, as well as immune dysfunction is believed to be determinative in the development of ASD.5., 6.

Moreover, in about a quarter of ASD cases, transplacental maternal autoantibodies reacting with specific proteins in the fetal brain have been fingered as the trigger for the neurodevelopmental impairment seen in ASD.6., 7. The placental transfer of Immunoglobulin G (IgG)[8] isotype antibodies, mediated by neonatal Fc receptor (FcRn), is an evolutionary mechanism for short-term humoral immunity in the developing immunologically naïve fetus.[9] Further, during fetal development, the blood–brain barrier is permeable to maternal antibodies.[10] As such, maternal autoantibodies cross the placental barrier without much selectivity, exposing the fetal brain to potentially harmful agents. Braunschweig et al recently uncovered seven proteins in the fetal brain targeted by maternal autoantibodies: stress-induced phosphoprotein 1 (STIP1), lactate dehydrogenase (LDH) A and B, guanine deaminase (cypin), collapsin response mediator proteins (CRMPs) 1 and 2, and Y-box binding protein (YBX1). It remains unclear how these autoantibodies arise, but possible triggers postulated to play a role in autoantibody production are loss of self-tolerance, molecular mimicry, and genetic predisposition.[7] Regardless, several murine and rhesus monkey models have demonstrated that transfer of purified IgG from mothers of children with ASD induces long-term behavioral changes in gestationally-exposed offspring,

similar to that seen in human autism cases.11., 12., 13. Ostensibly, removal of these MAR autoantibodies may limit the development of MAR autism in infants.

Nanoparticle systems could provide a relatively simple and cost-effective option for prevention of MAR Autism. Nanoparticles composed of different nanostructures and compositions, including gold, graphene, silica, and iron, have demonstrated extensive applications in targeted drug delivery.[14] Among these, iron oxide nanoparticles (IONPs) have emerged as an excellent candidate for biomedical applications, primarily due to their desirable physical characteristics such as high surface area to volume ratio and inherent magnetism.[15] These qualities have impelled the use of IONPs in clinical magnetic resonance imaging (MRI) as a contrast agent and for separation of environmental contaminants.16., 17., 18. Additionally, magnetic hyperthermia, heating of magnetic nanoparticles non-invasively with alternating magnetic fields, has shown great promise in destroying tumor cells and could potentially be applied for the destruction of surface-bound, pathological autoantibodies.[19] Other advantageous characteristics of IONPs include biocompatibility, stability, cost-effectiveness, and eco-friendliness.[20] Notably, the Food and Drug Administrator (FDA) has approved IONPs for use as MRI contrast agents and iron deficiency supplements.[21] However, a number of recent reports on unexpected adverse effects of IONPs have dampened enthusiasm on the biomedical use of IONPs.[22]

To address these concerns, researchers have resorted to a number of approaches including surface modification with dextran for improved biocompatibility and stability. Dextran iron oxide nanoparticles (DIONPs) are remarkably non-immunogenic.[23] Further, the addition of polyethylene glycol (PEG) surface-coating limits opsonization and phagocytic uptake by macrophages, thereby promoting longer blood circulation times.[24] Surface-decoration of DIONPs with cancer-homing peptides has prompted the development of targeted cancer therapeutics and novel MRI contrast agents.25., 26. Paralleling these technologies, we aim to develop a MAR LDH B epitope surface-functionalized dextran iron oxide-based nanoparticle therapeutic to act as a biomagnetic scavenger that circulates in the maternal blood and clears malicious autoantibodies before they can reach the fetal brain. This epitope-functionalized formulation is rationally designed to prevent non-specific protein adsorption, while capturing MAR autoantibodies with high specificity and affinity. We selected this LDH B epitope as it is observed exclusively in the mothers of children with ASD with relatively high prevalence.[27] In this capacity, this LDH B epitope-functionalized nanoparticle system will serve as a proof of concept for sequestration of MAR autoantibodies. Given the concerns on administration of iron oxide nanoparticles to pregnant women, we performed preliminary *in vitro* and *in vivo* toxicity assessments. Moreover, this platform is generalizable to other immune conditions with similar pathogenesis, such as *Erythroblastosis Fetalis*, where fetal and maternal blood type incompatibility results in the destruction of fetal Red Blood Cells (RBCs).

Methods

We synthesized ~15 nm dextran DIONPs (Figure 1) similar to Jarret et al coprecipitation method[28] with the modification of adding non-reduced dextran (*Leuconostoc mesenteroides*; average MW: 9000–11,000; Sigma Aldrich, St. Louis, MO). Next, DIONPs were surface-

decorated with citric acid (CA) (Sigma Aldrich, St. Louis, MO) to add carboxyl groups on the surface for further modification. Further, we added Methoxy PEG amine (10 kDa) (PolySciences, Warrington, PA) at 10:1 ratio (% w/w) to amine reactive DIO-CA NPs *via* carbodiimide chemistry. We physico-chemically characterized the DIONPs using DLS, FTIR, XRD, and TGA (Supplementary). *In vitro* and *in vivo* experimental details are extensively described in the 'Supplementary' section.

Results

Nanoparticle synthesis and characterization

Transmission electron microscopy and DLS analysis of the DIONPs demonstrated uniform particle shape and size. The average hydrodynamic diameter of NPs, measured by DLS, was 15 nm (Figure 2, A-B). X-ray Powder Diffraction (XRD) for DIONPs confirm crystalline structure in accordance with Fe_3O_4 magnetite standard, JCPDS card no. 85–1436 (Supplementary Figure S1, A).[29] There were no differences in the 2-theta position of the peaks compared to the standard, validating the crystalline structure. To confirm the presence of dextran, citric acid, and methoxy PEG (10 kDa) amine surface moieties, FTIR spectroscopy was performed on different DIONP formulations and relevant controls (Figure 2, C). The presence of a characteristic broad peak at 3257 cm^{-1} corresponded to the –OH bond of dextran and a sharp peak at 1097 cm^{-1} and 1349 cm^{-1} corresponded to the vibration band (asymmetric stretch) of O-CH_2 ether bond of methoxy PEG amine.[30] Additionally, adsorption bands at 1251 cm^{-1} and 1472 cm^{-1} associated with the –CH_2 vibration of the PEG, while peaks at 1400 and 1600 cm^{-1} corresponded to symmetric stretching of COO^-.[31] These unique peaks identifying functional groups matched with those of the crude materials shown on the bottom three spectra and confirmed the addition of methoxy PEG amine and CA on the DIONPs.

To further prove the presence of PEG of the NPs, we assessed the surface charge for the different DIONP formulations at various pHs (Figure 2, D). We hypothesized that PEGylated DIONPs would have more stable surface charges when incubated in different pH solutions than non-PEG coated DIONPs. PEG surface functionalization results in fewer carboxyl groups which are very susceptible to deprotonation as the pH is increased. In general, we observed a reduction in NP zeta potential as the solution pH was increased, signaling deprotonation of surface hydroxyl and carboxyl groups. Unsurprisingly, DIO-CA NPs demonstrated the greatest decline in zeta potential due to the high surface density of citric acid moieties. The PEG-coated NPs, with fewer carboxyl groups, exhibited greater resistance to surface charge diminution with increased pH, further confirming the presence of PEG on the surface of the NPs.

Addition of organic matter (LDH B peptide) was also confirmed based on thermogravimetric analysis. The TGA weight loss, corrected for the oxidation of the divalent iron, is equal to the total amount of all organic molecules on the nanoparticle surface. The weight loss increases with the content of organic molecules increase because of the change in the magnetite nanoparticle/coatings ratio. The weight percentage of the magnetite in the methoxy PEG amine NPs is 68.02 wt% and drops to around 64.69 wt% for the LDH-B peptide coated NPs, which gives approximately 3.33 wt% peptide in the LDH-B peptide

coated NPs (Supplementary Table 1 and Figure S1, B). The final product of each TG-DSC experiment was verified using XRD and FTIR (not shown) and found to be pure α-Fe_2O_3, which indicates a complete oxidation of the magnetite nanoparticle.[32]

Nanoparticle aggregation and adsorption assay

Figure 3, A shows that we observed only modest aggregation of the different NPs in various aqueous media. On average, aggregated particles demonstrated a hydrodynamic diameter of approximately 150 nm. Further, we demonstrated that the DIONPS surface-conjugated with PEG, of 10 kDa and 20 kDa MWs, significantly limited surface adsorption of BSA, even at a physiologically-relevant BSA concentration of 50 mg/ml (Figure 3, B). Based on this result and other literature, we used the 10 kDa PEG for the SNARE formulation in the subsequent studies.65., 33.

MAR peptide conjugation to DIONPs

Lactate dehydrogenase B peptide was surface conjugated to NPs *via* an EDC/NHS reaction. To verify conjugation and determine the surface density of the peptide, the LDH B peptide was outfitted with a fluorophore (FITC) at the N-terminal and a chymotrypsin cleavable domain proximal to the N terminus of the peptide. Based on analysis of the FITC fluorescence in the supernatant, following enzymatic cleavage and removal of NPs, we quantified a peptide surface density of 33.8 μg peptide/cm^2, which corresponds to a conjugation efficiency of approximately 70% (Figure 3, C). Additionally, nanoparticle aggregation and adsorption assays were repeated for SNAREs (Supplementary Figure S2).

Evaluation of cell viability and NP cellular uptake by macrophages

By flow cytometric analysis, double-positive results for PI and CD11b were used to determine the percent of viable cells. Based on our observations, the LC25 (the concentration at which 25% lethality is observed) for SNAREs was an NP concentration of ~500 μg/ml (Figure 3, D). Further, we observed a significantly lower macrophage uptake of SNAREs compared to the DIONPs and CA-DIONPs at 1 and 2 h incubation times at 37 °C (Figure 4, A-B).

Phenotypic analysis of dendritic cells and macrophages

We report the expression of maturation markers on innate immune cells as a composite maturation index (CMI),[34] an unweighted average of relative expressions of CD80, CD86, and MHC II. Our studies demonstrated no significant change in the CMI for DCs and macrophages (Macs) treated with DIONPs or SNAREs compared to immature DCs or Macs (Figure 5, A-B). Further, we investigated anti-inflammatory IL-10 and pro-inflammatory IL-12 cytokine secretion by bone marrow-derived DCs in presence of DIONPs and SNAREs (Supplementary Figure 3). In comparison to LPS-treated DCs, IL-12 secretion is substantially diminished in SNARE-treated DCs at both time points assessed (Supplementary Figure S3, A). Seemingly, our SNAREs, do not elicit innate immune cell activation.

In vitro assessment of complement activation–C5a generation

We observed a significant elevation in C5a concentration of DIONP-treated (0.5 mg/ml) serum and zymosan-treated samples compared to saline-treated, or samples incubated with SNAREs (0.5 mg/ml). Interestingly, our studies showed no significant change in C5a concentration for SNAREs compared to saline control (Figure 5, C). This result indicates that our SNARE formulation does not activate the complement system.

Assessment of MAR autoantibody capture, specificity, and avidity *in vitro*

In vitro, we demonstrated entrapment up to 2.7 μg LDH B Ab/ mg SNAREs (95% efficiency) from aqueous solution (Figure 6, A). Isotype control primary antibodies were used as negative controls (Supplementary Figure S4). Moreover, we demonstrated that SNAREs (0.25 mg/ml) reduced the LDH B antibody titer in human serum by ~ 90% (Figure 6, B). Isotype controls along with standard antibody titer dilutions were again used to qualify these results (Supplementary Figure S5). Additionally, scrambled LDH B epitope versions of SNAREs and naked DIONPs were used as controls and demonstrated minimal capturability. Further, LDH B antibody avidity for the SNAREs, in the presence of sodium thiocyanate, to have a 50% Avidity Index (AI) at 3.6 M chaotrope concentration (Figure 6, C). Antibody controls in the chaotrope solution are demonstrated in Supplementary Figure S6 and showed no functional changes compared to the PBS control.

SNARE maximum tolerated dose (MTD) and assessment of complement activation in pregnant dams

Central to the translation of this SNARE therapeutic, we determined the maximum tolerated dose (MTD) in pregnant dams. We intravenously administered SNAREs to C57BL/6j mice at different dosages, which were based on the *in vitro* cytotoxicity studies shown above (Figure 3, D). Due to mortality in mice treated with 300 mg NPs/kg dose ($n = 3$; mortality upon injection) and no overt toxicity at 150 mg NPs/kg, we established the maximum tolerated dose at 150 mg NPs/kg body mass. Maternal weight, tracked from GD 0 to GD 12, confirmed pregnancy and showed a significant increase in maternal weight compared to non-pregnant mice (Supplementary Figure S7, A; Table S1). In addition, there was no significant difference in maternal weight gain (calculated by subtracting the weight of the dam at GD 0 and uteri from the weight of the dam at GD 17) among the treatment groups and saline control (Supplementary Figure S7, B). Further, maternal weight after injection of SNAREs on GD 12 to GD 17 exhibited no significant change apart from the general weight increase due to pregnancy compared to saline-administered controls (Figure 7, A). There were no significant differences observed for average fetal weight and frequency of fetal resorption (Figure 7, B-C; Supplementary Table S1) for any of the administered SNARE dosages, indicating no harmful effects to maternal and fetal health. Further, we observed no significant change in the serum concentration of C5a and C5b-9 of mice treated with SNAREs compared to the saline-treated control (Figure 7, D-E). Minimal to no histological abnormalities were observed for the SNARE treatment groups up to 15 mg NPs/kg. In the 30 mg NPs/kg SNARE and DIONP treatment groups, brown intracytoplasmic pigment was present in the occasional Kupffer cells with no evidence of hepatocellular damage. In the kidney, the lumina of rare glomerular capillaries were occluded by similar material. In the

same groups, brown, homogeneous, round to oval aggregated iron deposits were present within the lumina of pulmonary capillaries. The occurrence of these particles in the pulmonary parenchyma was rare and no pathologic changes such as infarction or inflammation were associated with their presence.

In the maximal dose of 150 mg NPs/kg, lung was the tissue with maximal amount of intravascular brown homogeneous material (indicative of iron deposits). The presence of this material in the lung is sometimes associated with a mild degree of congestion of the pulmonary vasculature. In the liver, the iron deposits were primarily observed within the Kupffer cells at moderate to high frequency (Figure 8). In the kidney, the brown pigment was present with in glomerular capillaries and occasionally in the renal venules. Despite the presence of iron deposits in the lung, kidney, and the Kupffer cells in the liver, no pathological changes were observed in the organs from animals in this group.

Discussion

Deeper understanding of the pathogenesis of MAR Autism, a disease with rising prevalence, has given immunoengineers an opportunity to develop a prophylactic against MAR autism. Treatment of this complex disease, involving the transplacental movement of inflammatory autoantibodies, calls for an innovative approach that would eliminate pathological antibodies prior to fetal brain interaction. Our proposed solution is to deploy magnetic NPs that circulate throughout the maternal blood circuitry, conjugate and sequester the disease-causing autoantibodies, and thereby diminish their propensity to reach the fetal brain. The rational design of this system has to account for multiple physico-chemical parameters, if there is to be successful enactment of this technology — coined SNAREs. Based on reported inferences, some critical parameters for successful biomedical application of this nanotechnology include (1): the ability to prevent non-specific protein adsorption (2); specifically target the pathological autoantibodies; and (3) minimize phagocytic uptake/ increase circulation half-life.

To satisfy these constraints, we first synthesized DIONPs which have been identified in previous works for prolonged blood stability, biocompatibility, ease of fabrication, and surface-modification ability.[20] Next, we addressed NP dispersibility in biological media, which is pertinent to prevention of NP aggregation and reduced risk of blood vessel occlusion. We prepared DIONPs roughly 15 nm in diameter and then modified their surfaces with citric acid to provide the carboxyl groups for binding methoxy PEG amine. We investigated the effect of different size PEGs (750 Da, 10 kDa, and 20 kDa) on nanoparticle aggregation and non-specific protein adsorption. After overnight incubation of various PEGylated DIONPs and SNAREs, we observed no substantial NP aggregation. Generally, particle aggregates remained below 200 nm in diameter. This modest aggregation is physiologically acceptable, as NP aggregate size falls considerably lower than the diameter of the smallest capillaries at a few micrometers[35] and doesn't pose a risk of initiating thrombosis or blood vessel occlusion.[36] Particle aggregation may also limit accessibility of pathological autoantibodies to the surface-functionalized peptides, and could also promote clearance of the NPs, and therefore hinder the desired function of the SNAREs. Ostensibly,

this is an important parameter for maintaining any antibody entrapment potency of the SNARE system.

Another criterion for the nanoparticle design was the ability to deter binding of non-specific proteins, and therefore maximize exposure of peptide-binding sites to MAR autoantibodies. To enable specific binding of nanoparticles to MAR autoantibodies, as well as prevent unwanted uptake by immune phagocytic cells, we surface-modified the NPs with PEG chains. As established in previous literature, PEG introduces steric hindrance and interactions that prevent non-specific protein adsorption, thereby allowing only stronger interactions, such as antibody–epitope binding, to persist.[37] This behavior has been attributed to the ability of PEG chains to form a hydrophilic, hydrated shell around the NP and also results in less recognition by phagocytic cells.[38] To validate our hypothesis that NP PEGylation would reduce non-specific protein binding, we incubated the DIONPs and SNAREs in different concentration of BSA solutions (5, 10, and 50 mg/ml PBS) overnight. Consistent with other reports, we observed significantly lower BSA adsorption by PEG 10 kDa and 20 kDa surface-coated nanoparticles compared to controls.39., 40., 41. Interestingly, for these two formulations, we observed high levels of repulsion of BSA at 50 mg/ml BSA, which is comparable to the concentration of protein in the blood (60–80 mg/ml).[42] PEGylation not only hindered protein adsorption, but also disrupted NP uptake by phagocytic cells. When peptide-functionalized PEG (10 kDa)-coated DIONPs were incubated with macrophages, we observed significant reduction of NP uptake by macrophages compared to DIONPs and CA-DIONPs after 1 h of incubation, further corroborating multiple studies in literature.24., 43.

Progressing towards the development of a System for Nanoparticle-based Autoantibody Retention and Entrapment (SNARE), we demonstrated SNAREs removed up to 95% of LDH B antibodies from aqueous solution (~2.7 μg Ab/ mg NP). This would equate to the binding capacity of ~405 μg of Ab for the maximum *in vivo* tolerated dose of 150 mg NPs/kg (25.11 mg of LDH B Ab capture capacity in an adult human). The total IgG1 concentration in human serum is estimated at 4.48 mg/ml (~22.4 g/5 l total blood volume). In mothers of unborn, autistic offspring, the LDH B blood content would be a small fraction of this total concentration, which is typically composed of a large repertoire of different Abs ($\sim 10^{12}$).[44] Clearly, our SNAREs have significant capacity to capture MAR Abs from the blood. This promising result motivated us to assess SNARE capture-ability of autoantibodies in more complex biological medium — human serum. Although in static conditions overnight, our SNARE formulation reduced the LDH B antibody titer in human serum by as much as 90%, for the maximal NP concentration tested. Further, our results exhibited increasing capture-ability with higher SNARE concentration. Additionally, we determined the avidity of the MAR LDH B antibody for the SNAREs and demonstrated the 50% AI at 3.6 M sodium thiocyanate chaotrope concentration, one of the most commonly used chaotropic salts. Similarly, Dauner et al developed an ammonium thiocyanate-modified ELISA to measure avidity of anti-HPV antibodies for its antigen.[45] However, they reported a 50% AI at 2 M ammonium thiocyanate solution. The MAR LDH B antibody's higher avidity for its peptide target on the SNAREs and the stability of the antibody–antigen complex is desirable for our application to capture and retain the pathological MAR antibodies to ultimately clear from the blood.[46] These experiments provide concrete evidence on the

capacity of the SNARE system to specifically target and bind MAR autism-related antibodies from a complex mixture of blood proteins, including other antibodies. In a similar vein, Hu et al reported on biomimetic nanoparticles, composed of red blood cell membrane-derived vesicles fused with poly(lactic-co-glycolic) acid (PLGA) nanoparticles, that abrogated type II hypersensitivity reaction — an autoimmune disease where antibodies target healthy cells, such as red blood cells (RBCs).[47]

While our *in vitro* results provide credence for the application of SNAREs to capture autoantibodies with specificity and high capacity, recent studies have cast doubt on the safe use of iron oxide nanoparticles in humans.[48] To allay these concerns, we assessed the toxicity of SNAREs *in vitro* and *in vivo*. Our LC25 concentration of 500 at μg/ml on *in vitro* viability was consistent with other studies, such as Masoud et al whom reported ~10% HeLa and MCF-7 cell death at 100 μg/ml DIONP concentration after 6, 12, and 24 h incubation times.[49] Similarly, another study reported LC25 concentrations *via* MTT Assay at 500 μg/ml of superparamagnetic iron oxide nanoparticles after 3 h incubation with J774 cells.[50] The LC25 concentration determined by our viability study was used as an anchor for a subsequent *in vivo* study to resolve the Maximum Tolerated Dose (MTD) of SNAREs.

Multiple studies have investigated the toxicity of iron oxide nanoparticles *in vivo*, but the toxicity of dextran iron oxide nanoparticles after intravenous injection in pregnant mice has not been previously explored. Further, the small number of previous studies on DIONP toxicity has divergent conclusions, primarily due to differences in NP fabrication and study design parameters including routes of administration, nanoparticle size, surface composition, and surface charge. Bona et al investigated the toxicity of iron oxide NP surface-charge and dose on fetal development. Positively surface-charged Polyethyleneimine (PEI)-coated iron oxide NPs and negatively surface-charged poly(acrylic acid) (PAA)-coated NPs were intraperitoneally (IP) injected in pregnant CD-1 mice. The NP formulations were administered at a low (10 mg NPs/kg) and high (100 mg NPs/kg) dose on GD 8, 9, or 10 (critical window for organogenesis).[51] They noted no significant toxicity at the low dose for either formulation. However, at the higher dose they reported significant changes in the histology of uteri and testis. In another study, Noori et al IP-injected Dimercaptosuccinic acid (DMSA)-coated iron oxide nanoparticles in pregnant mice at 50, 100, 200, and 300 mg NPs/kg and demonstrated no major adverse effects on maternal weight changes. However, doses higher than 50 mg NPs/kg led to a significant decrease in the infant maturation after birth and 70% infant mortality before reaching puberty.[52] Comparing to our observed 150 mg NPs/kg tolerated dose, a number of aforementioned studies demonstrated significant toxicity at lower NP doses, such as IP-injected DMSA-IONPs at 50 mg NPs/kg[52] or IP-injected PEI/PAA-coated IONPs at 100 mg NPs/kg.[51] The incongruence between these studies and ours may be due to the non-immunogenic and biocompatible nature of dextran and PEG-coated iron oxide nanoparticles.23., 53. Further, surface charge is an important parameter in dictating toxicity level of NPs and more neutrally charged NPs produce low reactive oxidative species (ROS), thus exhibiting less toxicity.[54] Our SNAREs demonstrate a more neutral zeta potential at physiological pH 7 due to PEG and peptide surface moieties, which we suspect helps to mitigate NP toxicity *in vivo*. However, further studies are needed to assess the biodistribution, pharmacokinetics and chronic toxicity of SNAREs.

The pharmacokinetics and clearance of IONPs have been extensively explored in multiple studies. Generally, the main factors affecting pharmacokinetics performance are based on nanoparticle hydrodynamic size, surface coating, and administration route. Further, the principal clearance pathway of intravenously injections of IONPs is the mononuclear phagocytic system (MPS), consisting of phagocytic cells, followed by hepatic clearance. Importantly, blood half-life of IONPs is heavily dependent on the hydrodynamic diameter, ranging from several hours to days based on the injection dose and administration route.[8] Feng et al demonstrated NPs possessing diameter < 50 nm have been shown to benefit from slow opsonization and gradual clearance from the MPS.[24] Given our NP diameter of ~15 nm and surface-functionalization with PEG, we expect similar nanoparticle pharmacokinetics and slow clearance.[33] Ultimately, we believe our particles are metabolized in the liver and recycled back into many essential processes of the body, including energy metabolism, oxygen transport, and DNA synthesis.[55]

Significant concerns also surround the tendency of IONPs to activate inflammatory immune system mediators, particularly the complement system. For instance, Wolf-Grosse et al demonstrated significant increases in complement activation products C3a, C5a, and C5b-9 after 6 h of IONP incubation with human plasma at 10 μg/ml.[56] Additionally, other reports investigated *in vitro* complement activation of human and mouse serum with different types of iron oxide nanoparticles and demonstrated significant complement activation.57., 58. Given these reports and the desired application of the SNAREs, we investigated their proclivity to actuate the complement system. Interestingly, we found that there was a significant elevation of C5a in mouse serum exposed to DIONPs at 0.5 mg/ml, but not SNAREs. SNARE inability to activate the complement cascade is certainly advantageous and may be due to the incorporation of PEG. PEGylation prevents adsorption of plasma proteins (*e.g.* factor B) which play critical roles in the alternative and other complement activation pathways.[59]

We also assessed chronic complement factor activation *in vivo*, by measuring C5a and C5b-9 concentrations in serum of pregnant mice treated with SNAREs. Serum was obtained from mice on GD 17, five days after intravenously injecting SNAREs on GD 12. We found no significant change in C5a or C5b-9 serum concentrations for the different SNARE dosages compared to the saline and DIONP controls. Although complement activation is thought to occur early in the immune response to foreign entities, reports have demonstrated that head-injured mice retained significantly higher C5a levels up to 7 days after injury,[60] indicating that continuous complement activation is possible with persistent inflammatory cues. Interestingly, we demonstrated DIONPs significantly elevate C5a concentration in fresh mouse serum. But, there is an absence of a chronic C5a complement activation of mice treated with DIONPs. Taken together these results indicate that there is complement activation in the presence of DIONPs, but as these NPs are cleared, complement activation subsides. This result lays bare the potent effects of altering the potential contact points of nanotechnology with biological media.

If administered NPs are able to avoid a complement-mediated immune response, the next trial they face from the immune system is typically phagocyte interception and activation. Therefore, for our application, it is important that SNAREs limit the interaction, as well as

activation of these specialized immune cells. We investigated the ability of SNAREs and relevant controls to induce maturation in bone marrow-derived DCs and macrophages. Dendritic cells, dubbed as professional antigen-presenting cells (APCs), have the ability to pinocytose and endocytose DIONPs.[61] More importantly, other researchers have demonstrated that iron oxide nanoparticles can upregulate MHC II, CD40, CD86, and CCR7 on DCs after 12 h of co-incubation.[61] Contrary to this finding, we observed no significant change in DC or macrophage maturation markers for DIONP or SNARE treatments after 24 and 48 h incubation periods. Interestingly, we detected a significant increase in IL-12 production by DCs in presence of DIONPs compared to untreated DCs. Contrastingly, SNARE incubation with DCs did not stimulate significant IL-12 secretion. This is important as innate immune cell maturation can elicit activation of the adaptive immune system and generation of antibodies, as reported with adjuvant-coated IONPs.[62] The reduced immune cell maturation may be due to the presence of dextran, which others have reported can reduce the immunogenicity of iron oxide NPs.[23] Additionally, PEG coating of iron oxide NPs can contribute to reduced immune activation.[24]

In conclusion, this work represents a first-generation prototype of a nanomedicine that we believe has huge promise for preventing autoimmune autism. The outcome of this study could not only lead the way for a preventative therapeutic for MAR autism, but possibly serve as a platform for filtering autoantibodies from blood to treat other forms of autoimmune diseases (*e.g. Erythroblastosis Fetalis*). However, we are acutely aware that many deficiencies still exist for this system, and further optimization is required. Moreover, we plan to revisit parameters such as PEG length and surface density, and peptide surface concentration in order to fine tune our nanoparticle system. Future studies will also delve into the pharmacokinetics and biodistribution of SNAREs, as well as thoroughly explore the fetal and maternal toxicity of SNARES in pregnant mice. Once the formulation is optimized, we aim to assess the therapeutic efficacy of SNAREs in an existing autism mouse model.[63] We believe we have taken a critical first step to developing the first preventative therapeutic for ASD, a disorder expected to levy a $1 trillion burden on the economy by 2025.[3]

Supplementary Material

Refer to Web version on PubMed Central for supplementary material.

Acknowledgment

We would like to thank Dr. Joel Garcia for helping with the nanoparticle fabrication and Mr. Charles M. Smith for helping with I.V. injections of nanoparticles in pregnant dams.

Funding

AB was supported by the Floyd and Mary Schwall Dissertation Year Fellowship in Medical Research; AB and JSL were supported by a National Institutes of Health (NIH), National Institute of General Medical Sciences grant (grant number: R35GM125012).

References

1. DSM-5 autism spectrum disorder fact sheet. Association AP. 2013.

2. Christensen DL, Baio J, Van Naarden Braun K., Bilder D, Charles J, Constantino JN, et al.Prevalence and characteristics of autism Spectrum disorder among children aged 8 years—autism and developmental disabilities monitoring network, 11 sites, United States, 2012 MMWR Surveill Summ, 65 (3) (2016), pp. 1–23

3. Leigh JP, Du J. Brief report: forecasting the economic burden of autism in 2015 and 2025 in the United States J Autism Dev Disord, 45 (12) (2015), pp. 4135–4139 [PubMed: 26183723]

4. DeFilippis M, Wagner KD Treatment of autism spectrum disorder in children and adolescents Psychopharmacol Bull, 46 (2) (2016), pp. 18–41 [PubMed: 27738378]

5. Onore C, Careaga M, Ashwood P. The role of immune dysfunction in the pathophysiology of autism Brain Behav Immun, 26 (3) (2012), pp. 383–392 [PubMed: 21906670]

6. Jones KL, Van de Water J. Maternal autoantibody related autism: mechanisms and pathways Mol Psychiatry, 24 (2) (2019), pp. 252–265 [PubMed: 29934547]

7. Fox-Edmiston E, Van de Water J. Maternal anti-fetal brain IgG autoantibodies and autism spectrum disorder: current knowledge and its implications for potential therapeutics CNS Drugs, 29 (9) (2015), pp. 715–724 [PubMed: 26369920]

8. Arami H, Khandhar A, Liggitt D, Krishnan KM In vivo delivery, pharmacokinetics, biodistribution and toxicity of iron oxide nanoparticles Chem Soc Rev, 44 (23) (2015), pp. 8576–8607 [PubMed: 26390044]

9. Braunschweig D, Ashwood P, Krakowiak P, Hertz-Picciotto I, Hansen R, Croen LA, et al.Autism: maternally derived antibodies specific for fetal brain proteins Neurotoxicology, 29 (2) (2008), pp. 226–231 [PubMed: 18078998]

10. Kowal C, DeGiorgio LA, Nakaoka T, Hetherington H, Huerta PT, Diamond B, et al.Cognition and immunity; antibody impairs memory Immunity, 21 (2) (2004), pp. 179–188 [PubMed: 15308099]

11. Braunschweig D, Golub MS, Koenig CM, Qi L, Pessah IN, Van de Water J, et al.Maternal autism-associated IgG antibodies delay development and produce anxiety in a mouse gestational transfer model J Neuroimmunol, 252 (1–2) (2012), pp. 56–65 [PubMed: 22951357]

12. Singer HS, Morris C, Gause C, Pollard M, Zimmerman AW, Pletnikov M. Prenatal exposure to antibodies from mothers of children with autism produces neurobehavioral alterations: a pregnant dam mouse model J Neuroimmunol, 211 (1–2) (2009), pp. 39–48 [PubMed: 19362378]

13. Martin LA, Ashwood P, Braunschweig D, Cabanlit M, Van de Water J, Amaral DG Stereotypies and hyperactivity in rhesus monkeys exposed to IgG from mothers of children with autism Brain Behav Immun, 22 (6) (2008), pp. 806–816 [PubMed: 18262386]

14. Petros RA, DeSimone JM Strategies in the design of nanoparticles for therapeutic applications Nat Rev Drug Discov, 9 (8) (2010), pp. 615–627 [PubMed: 20616808]

15. Stephen ZR, Kievit FM, Zhang M. Magnetite nanoparticles for medical MR imaging Mater Today (Kidlington), 14 (7–8) (2011), pp. 330–338 [PubMed: 22389583]

16. Wu W, Wu Z, Yu T, Jiang C, Kim WS Recent progress on magnetic iron oxide nanoparticles: synthesis, surface functional strategies and biomedical applications Sci Technol Adv Mater, 16 (2) (2015), Article 023501

17. Tang T, Valenzuela A, Petit F, Chow S, Leung K, Gorin F, et al.In vivo MRI of functionalized Iron oxide nanoparticles for brain inflammation Contrast Media Mol Imaging, 2018 (2018), p. 3476476

18. Tu C, Ng TS, Sohi HK, Palko HA, House A, Jacobs RE, et al.Receptor-targeted iron oxide nanoparticles for molecular MR imaging of inflamed atherosclerotic plaques Biomaterials, 32 (29) (2011), pp. 7209–7216 [PubMed: 21742374]

19. Banobre-Lopez M, Teijeiro A, Rivas J. Magnetic nanoparticle-based hyperthermia for cancer treatment Rep Pract Oncol Radiother, 18 (6) (2013), pp. 397–400 [PubMed: 24416585]

20. Lu AH, Salabas EL, Schuth F. Magnetic nanoparticles: synthesis, protection, functionalization, and application Angew Chem Int Ed Engl, 46 (8) (2007), pp. 1222–1244 [PubMed: 17278160]

21. Lu M, Cohen MH, Rieves D, Pazdu R. FDA report: Ferumoxytol for intravenous iron therapy in adult patients with chronic kidney disease Am J Hematol, 85 (5) (2010), pp. 315–319 [PubMed: 20201089]

22. Ghasempour S, Shokrgozar MA, Ghasempour R, Alipour M. Investigating the cytotoxicity of iron oxide nanoparticles in in vivo and in vitro studies Exp Toxicol Pathol, 67 (10) (2015), pp. 509–515 [PubMed: 26279467]

23. Unterweger H, Janko C, Schwarz M, Dezsi L, Urbanics R, Matuszak J, et al.Non-immunogenic dextran-coated superparamagnetic iron oxide nanoparticles: a biocompatible, size-tunable contrast agent for magnetic resonance imaging Int J Nanomedicine, 12 (2017), pp. 5223–5238 [PubMed: 28769560]
24. Feng Q, Liu Y, Huang J, Chen K, Huang J, Xiao K. Uptake, distribution, clearance, and toxicity of iron oxide nanoparticles with different sizes and coatings Sci Rep, 8 (1) (2018), p. 2082 [PubMed: 29391477]
25. Kruse AM, Meenach SA, Anderson KW, Hilt JZ Synthesis and characterization of CREKA-conjugated iron oxide nanoparticles for hyperthermia applications Acta Biomater, 10 (6) (2014), pp. 2622–2629 [PubMed: 24486913]
26. Sulek B.M. Selim, DavutMahcicek I, Sozeri Huseyin, Atalar Ergin, Tekinaya Ayse B. and Guler Mustafa O.. Peptide functionalized superparamagnetic iron oxide nanoparticles as MRI contrast agents, 39 (2011)
27. Edmiston E, Jones KL, Vu T, Ashwood P, Van de Water J. Identification of the antigenic epitopes of maternal autoantibodies in autism spectrum disorders Brain Behav Immun, 69 (2018), pp. 399–407 [PubMed: 29289663]
28. Jarrett BR, Frendo M, Vogan J, Louie AY Size-controlled synthesis of dextran sulfate coated iron oxide nanoparticles for magnetic resonance imaging Nanotechnology, 18 (3) (2007), Article 035603
29. Cao X, Wang W, Zhang X, Li L, Cheng Y, Liu H, et al.Magnetic properties of fluffy Fe@alpha-Fe2O3 core-shell nanowires Nanoscale Res Lett, 8 (1) (2013), p. 423 [PubMed: 24134440]
30. Gupta AK, Wells S. Surface-modified superparamagnetic nanoparticles for drug delivery: preparation, characterization, and cytotoxicity studies IEEE Trans Nanobioscience, 3 (1) (2004), pp. 66–73 [PubMed: 15382647]
31. Yan X, Huang X, Yu C, Deng H, Wang Y, Zhang Z, et al.The in-vitro bioactivity of mesoporous bioactive glasses Biomaterials, 27 (18) (2006), pp. 3396–3403 [PubMed: 16504289]
32. Nuhn L, Vanparijs N, De Beuckelaer A, Lybaert L, Verstraete G, Deswarte K, et al.pH-degradable imidazoquinoline-ligated nanogels for lymph node-focused immune activation Proc Natl Acad Sci U S A, 113 (29) (2016), pp. 8098–8103 [PubMed: 27382168]
33. Jokerst JV, Lobovkina T, Zare RN, Gambhir SS Nanoparticle PEGylation for imaging and therapy Nanomedicine (Lond), 6 (4) (2011), pp. 715–728 [PubMed: 21718180]
34. Suk JS, Xu Q, Kim N, Hanes J, Ensign LM. PEGylation as a strategy for improving nanoparticle-based drug and gene delivery. Adv Drug Deliv Rev. 2016;99(Pt A):28–51. [PubMed: 26456916]
35. Lewis JS, Roche C, Zhang Y, Brusko TM, Wasserfall CH, Atkinson M, et al.Combinatorial delivery of immunosuppressive factors to dendritic cells using dual-sized microspheres J Mater Chem B, 2 (17) (2014), pp. 2562–2574 [PubMed: 24778809]
36. Lowe James S.. Stevens & Lowe's human histology (fourth edition), chapter 9 — blood and lymphatic circulatory systems and heart 2015.
37. Nadziejko C, Fang K, Chen LC, Cohen B, Karpatkin M, Nadas A. Effect of concentrated ambient particulate matter on blood coagulation parameters in rats Res Rep Health Eff Inst, 111 (2002), pp. 7–29 discussion 31–8
38. Gustafson HH, Holt-Casper D, Grainger DW, Ghandehari H. Nanoparticle uptake: the phagocyte problem Nano Today, 10 (4) (2015), pp. 487–510 [PubMed: 26640510]
39. Branca SM C, Maisano G, Migliardo F, Migliardo P, Romeo G.. Hydration study of PEG/water mixtures by quasi elastic light scattering, acoustic and rheological measurements. J Phys Chem B 2002;106(2002):10272–6.
40. Copp JA, Fang RH, Luk BT, Hu CM, Gao W, Zhang K, et al.Clearance of pathological antibodies using biomimetic nanoparticles Proc Natl Acad Sci U S A, 111 (37) (2014), pp. 13481–13486 [PubMed: 25197051]
41. Yallapu MM, Foy SP, Jain TK, Labhasetwar V. PEG-functionalized magnetic nanoparticles for drug delivery and magnetic resonance imaging applications Pharm Res, 27 (11) (2010), pp. 2283–2295 [PubMed: 20845067]
42. Kang KGNaET. Functionalization of inorganic nanoparticles with polymers for stealth biomedical applications. Polymer Chemistry 2010.

43. Anderson NL, Anderson NGThe human plasma proteome: history, character, and diagnostic prospects Mol Cell Proteomics, 1 (11) (2002), pp. 845–867 [PubMed: 12488461]
44. Park YC, Smith JB, Pham T, Whitaker RD, Sucato CA, Hamilton JA, et al.Effect of PEG molecular weight on stability, T(2) contrast, cytotoxicity, and cellular uptake of superparamagnetic iron oxide nanoparticles (SPIONs) Colloids Surf B Biointerfaces, 119 (2014), pp. 106–114 [PubMed: 24877593]
45. Semenova VA, Steward-Clark E, Stamey KL, Taylor TH Jr., Schmidt DS, Martin SK, et al.Mass value assignment of total and subclass immunoglobulin G in a human standard anthrax reference serum Clin Diagn Lab Immunol, 11 (5) (2004), pp. 919–923 [PubMed: 15358653]
46. Dauner JG, Pan Y, Hildesheim A, Kemp TJ, Porras C, Pinto LA Development and application of a GuHCl-modified ELISA to measure the avidity of anti-HPV L1 VLP antibodies in vaccinated individuals Mol Cell Probes, 26 (2) (2012), pp. 73–80 [PubMed: 22285687]
47. Shityakov S, Salmas RE, Durdagi S, Salvador E, Papai K, Yanez-Gascon MJ, et al.Characterization, in vivo evaluation, and molecular modeling of different propofol-cyclodextrin complexes to assess their drug delivery potential at the blood-brain barrier level J Chem Inf Model, 56 (10) (2016), pp. 1914–1922 [PubMed: 27589557]
48. Hu CM, Zhang L, Aryal S, Cheung C, Fang RH, Zhang L.Erythrocyte membrane-camouflaged polymeric nanoparticles as a biomimetic delivery platform Proc Natl Acad Sci U S A, 108 (27) (2011), pp. 10980–10985 [PubMed: 21690347]
49. Valdiglesias V, Fernandez-Bertolez N, Kilic G, Costa C, Costa S, Fraga S, et al.Are iron oxide nanoparticles safe? Current knowledge and future perspectives J Trace Elem Med Biol, 38 (2016), pp. 53–63 [PubMed: 27056797]
50. Masoud Rezaei HM, Karim Khoshgard, Alireza Montazerabadi, Ahmad, Mohammadbeigi FO. The cytotoxicity of dextran-coated iron oxide nanoparticles on Hela and MCF-7 cancerous cell lines. Iranian Journal of Toxicology 2017;11(5):31–6.
51. Naqvi S, Samim M, Abdin M, Ahmed FJ, Maitra A, Prashant C, et al.Concentration-dependent toxicity of iron oxide nanoparticles mediated by increased oxidative stress Int J Nanomedicine, 5 (2010), pp. 983–989 [PubMed: 21187917]
52. Di Bona KR, Xu Y, Gray M, Fair D, Hayles H, Milad L, et al.Short- and long-term effects of prenatal exposure to iron oxide nanoparticles: influence of surface charge and dose on developmental and reproductive toxicity Int J Mol Sci, 16 (12) (2015), pp. 30251–30268 [PubMed: 26694381]
53. Noori K.P. Ali Modaresi Mehrdad, Messripour Manoochehr, Yousefi Mohamad Hasan and Amiri Gholam Reza. Effect of magnetic iron oxide nanoparticles on pregnancy and testicular development of mice Afr J Biotechnol, 10 (7) (2011), pp. 1221–1227
54. Yu M, Huang S, Yu KJ, Clyne AM Dextran and polymer polyethylene glycol (PEG) coating reduce both 5 and 30 nm iron oxide nanoparticle cytotoxicity in 2D and 3D cell culture Int J Mol Sci, 13 (5) (2012), pp. 5554–5570 [PubMed: 22754315]
55. Patil US, Adireddy S, Jaiswal A, Mandava S, Lee BR, Chrisey DB In vitro/in vivo toxicity evaluation and quantification of iron oxide nanoparticles Int J Mol Sci, 16 (10) (2015), pp. 24417–24450 [PubMed: 26501258]
56. Wang J, Pantopoulos K. Regulation of cellular iron metabolism Biochem J, 434 (3) (2011), pp. 365–381 [PubMed: 21348856]
57. Wolf-Grosse S, Rokstad AM, Ali S, Lambris JD, Mollnes TE, Nilsen AM, et al.Iron oxide nanoparticles induce cytokine secretion in a complement-dependent manner in a human whole blood model Int J Nanomedicine, 12 (2017), pp. 3927–3940 [PubMed: 28579778]
58. Wang G, Chen F, Banda NK, Holers VM, Wu L, Moghimi SM, et al.Activation of human complement system by dextran-coated iron oxide nanoparticles is not affected by dextran/Fe ratio, hydroxyl modifications, and crosslinking Front Immunol, 7 (2016), p. 418 [PubMed: 27777575]
59. Banda NK, Mehta G, Chao Y, Wang G, Inturi S, Fossati-Jimack L, et al.Mechanisms of complement activation by dextran-coated superparamagnetic iron oxide (SPIO) nanoworms in mouse versus human serum Part Fibre Toxicol, 11 (2014), p. 64 [PubMed: 25425420]
60. Moghimi SM, Simberg D. Complement activation turnover on surfaces of nanoparticles Nano Today, 15 (2017), pp. 8–10 [PubMed: 29399037]

61. Leinhase I, Rozanski M, Harhausen D, Thurman JM, Schmidt OI, Hossini AM, et al.Inhibition of the alternative complement activation pathway in traumatic brain injury by a monoclonal anti-factor B antibody: a randomized placebo-controlled study in mice J Neuroinflammation, 4 (2007), p. 13 [PubMed: 17474994]

62. Toki S, Omary RA, Wilson K, Gore JC, Peebles RS Jr., Pham W. A comprehensive analysis of transfection-assisted delivery of iron oxide nanoparticles to dendritic cells Nanomedicine, 9 (8) (2013), pp. 1235–1244 [PubMed: 23747738]

63. Neto LMMZN, de Sousa-Júnior, Trentini, da Costa, Bakuzis, Kipnis, et al.Specific T cell induction using iron oxide based nanoparticles as subunit vaccine adjuvant Hum Vaccin Immunother (2018), pp. 1–16 [PubMed: 29324170]

64. Judy Van de Water KLJ, Silverman Jill, Yang Mu, Crawley Jacqueline. Autism-specific maternal autoantibodies produce ASD relevant behaviors in a mouse model. Biol Psychiatry 2018;83(9):S147–S8.

65. Shityakov S, Salmas RE, Salvador E, Roewer N, Broscheit J, Forster C. Evaluation of the potential toxicity of unmodified and modified cyclodextrins on murine blood-brain barrier endothelial cells J Toxicol Sci, 41 (2) (2016), pp. 175–184 [PubMed: 26961601]

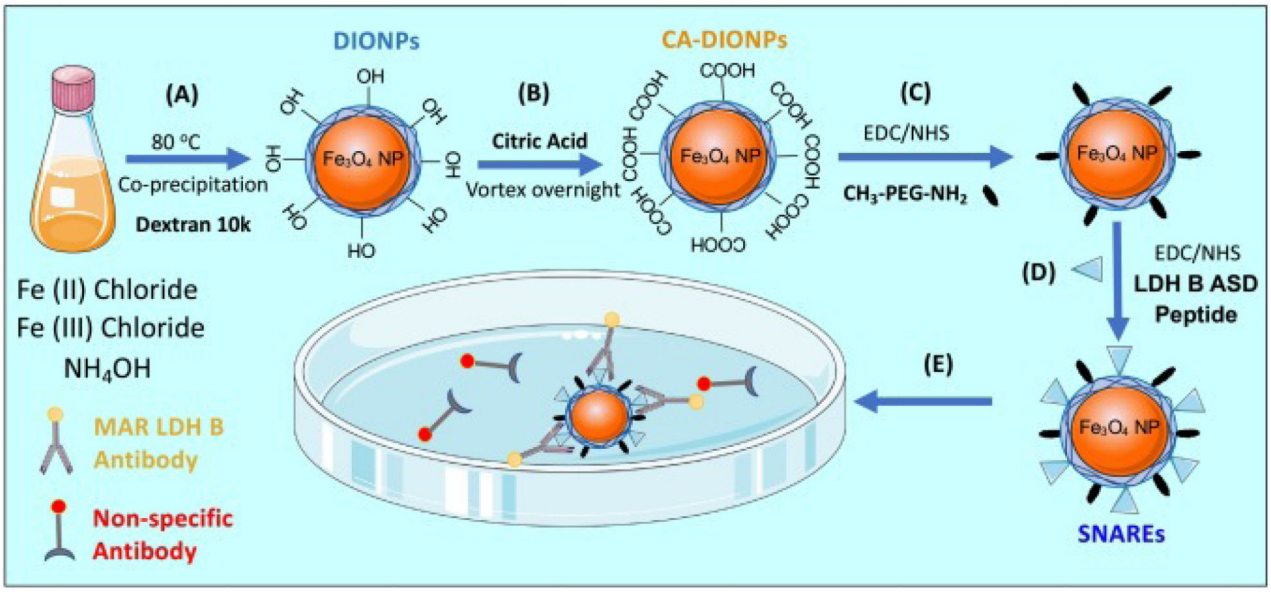

Figure 1.

Schematic summarizing synthesis of peptide-functionalized dextran iron oxide nanoparticles and capture of Autism-specific autoantibodies from an antibody solution. **(A)** Synthesis of dextran iron oxide nanoparticles (DIONPS) *via* co-precipitation method. **(B)** Exchange of DIONP surface hydroxyl groups with carboxylic groups by citric acid coating (DIO-CA NPs). **(C)** Nanoparticle surface-conjugation with Methoxy PEG Amine *via* EDC/NHS reaction (DIO-CA-PEG NPs). **(D)** Nanoparticle surface-decoration with LDH B ASD peptide *via* EDC/NHS Reaction (SNAREs). **(E)** SNAREs specifically ligate Anti-LDH B autoantibody from solution.

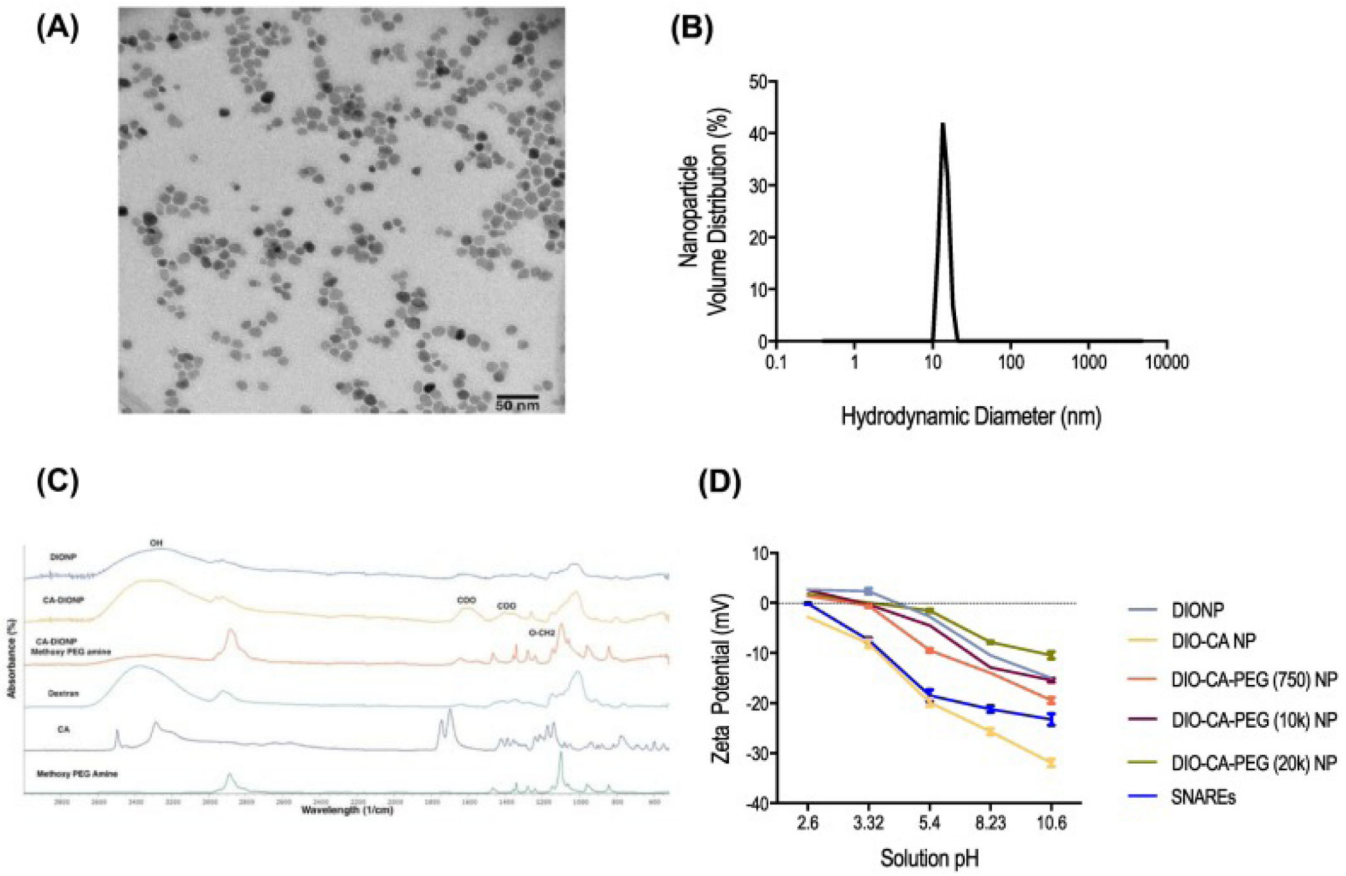

Figure 2.

SNARE physico-chemical characterization. **(A)** Transmission electron microscopy (TEM) of DIONPs. **(B)** Dynamic light scattering (DLS). **(C)** FTIR spectra of DIONPs, citric acid DIONPs, DIO-CA-PEG (10 kDa) NPs. **(D)** The zeta potential for naked DIONPs, DIO-CA NPs, and methoxy PEG amine (750 Da, 10 kDa, or 20 kDa)-coated DIO-CA NPs (1 mg/ml).

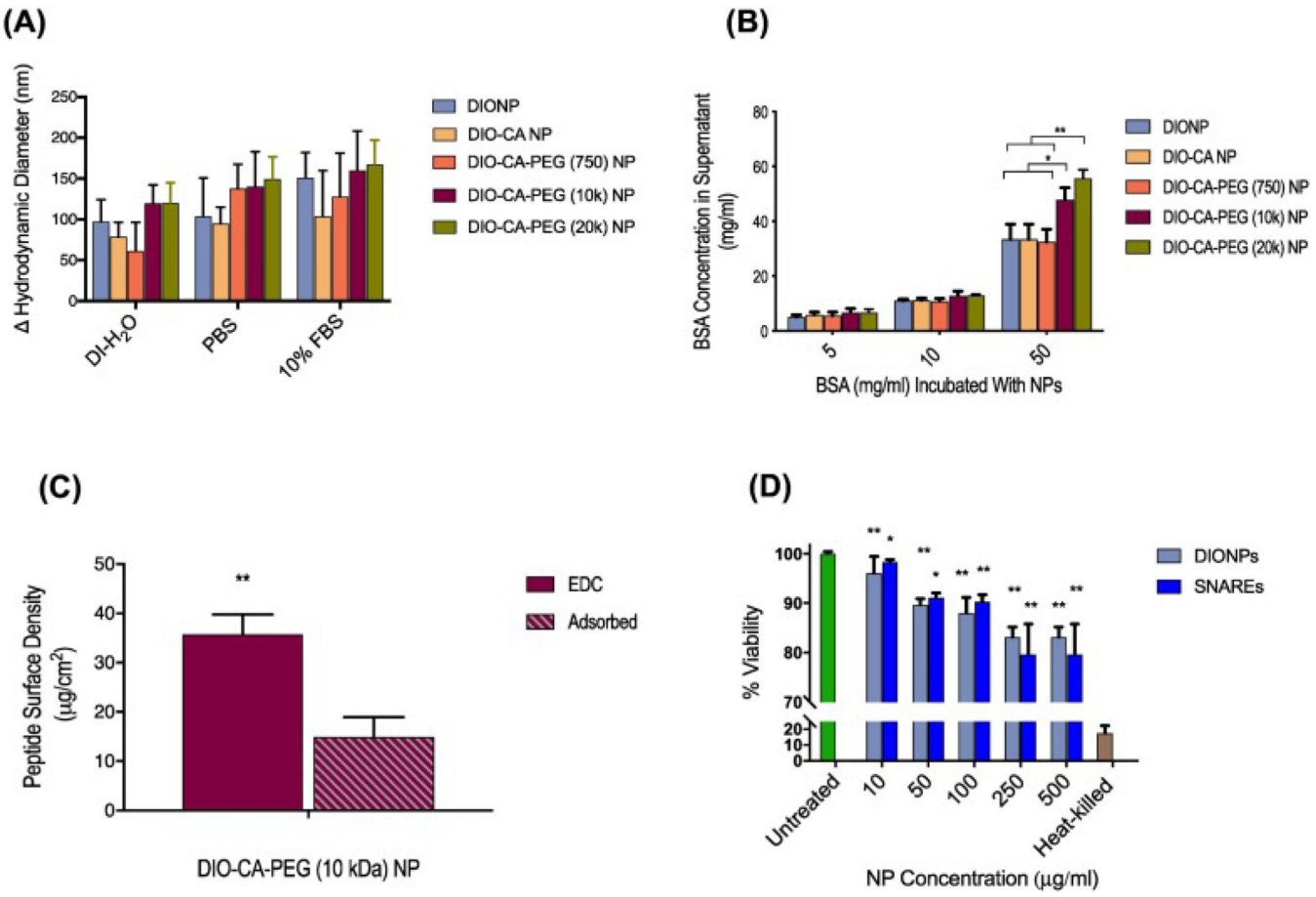

Figure 3.

Nanoparticle *in vitro* characterization and MAR peptide conjugation. **(A)** No significant nanoparticle aggregation was observed in various media (DI-H_2O, PBS, or 10% FBS in PBS) after 24 h incubation (measured using DLS). **(B)** PEG (10 kDa/ 20 kDa)-conjugated DIO-CA NPs had the highest repulsion ability, preventing adsorption of non-specific proteins (Bovine Serum Albumin [BSA]). BSA adsorption on DIONP formulations normalized to the number of DIONPs per batch. **(C)** Conjugation of FITC-LDH B peptide onto DIO-CA-PEG (10 kDa) NPs resulted in a final surface density of 33.8 μg peptide/cm^2. **(D)** *In vitro*, the LC25 for RAW 264.7 macrophage cells incubated with DIONPs and SNAREs was determined to be 500 μg/ml. Heat-killed and untreated cells were used as control and treatments normalized to untreated cells.[64]

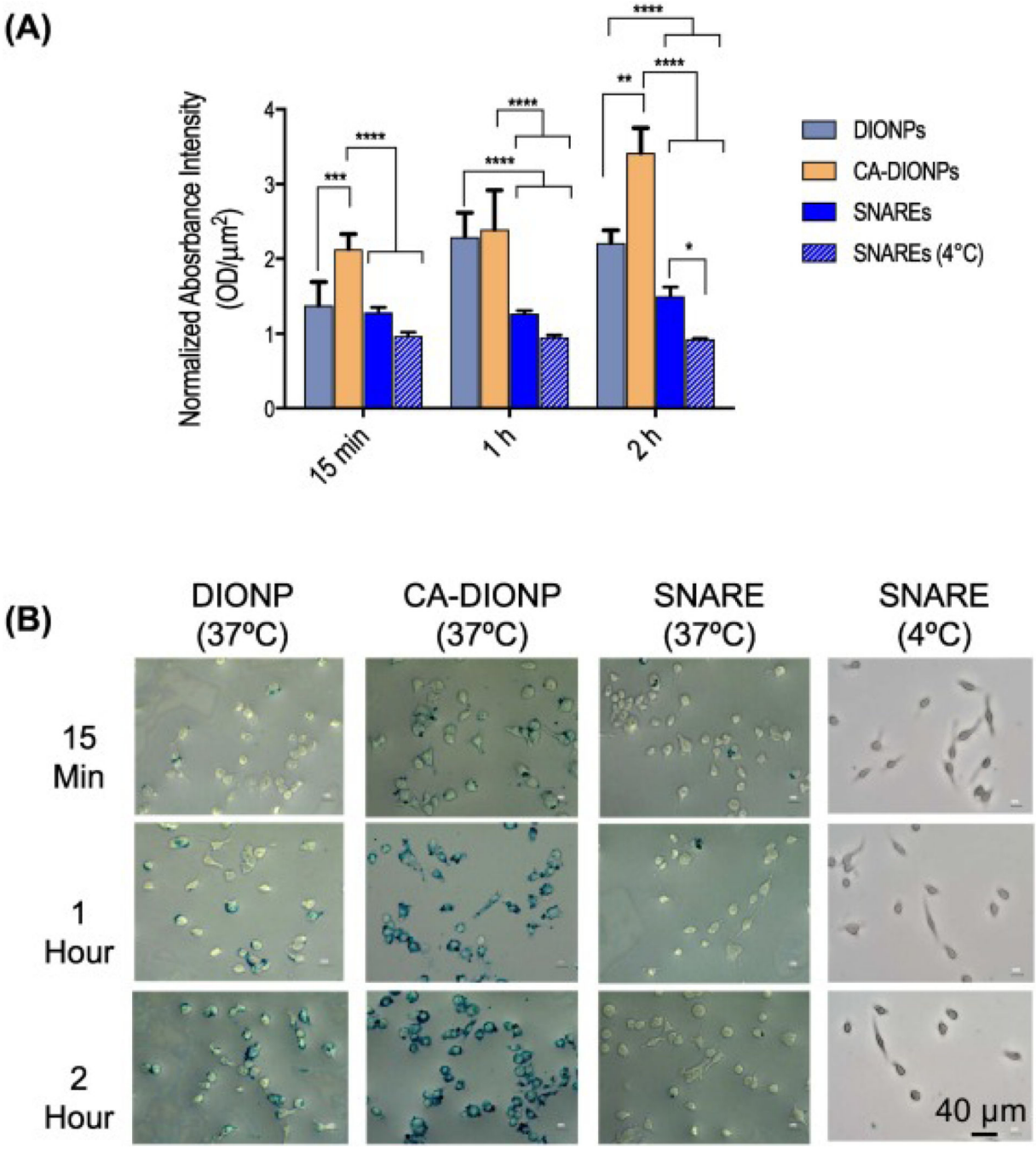

Figure 4.

Nanoparticle uptake by macrophages. **(A)** *In vitro* uptake of DIONPs, DIO-CA NPs, ad SNAREs by RAW 264.7 macrophages was assessed using a Prussian Blue iron stain after 15 min, 1 h, and 2 h of incubation at either 4 or 37 °C. **(B)** Representative images of Prussian Blue staining.

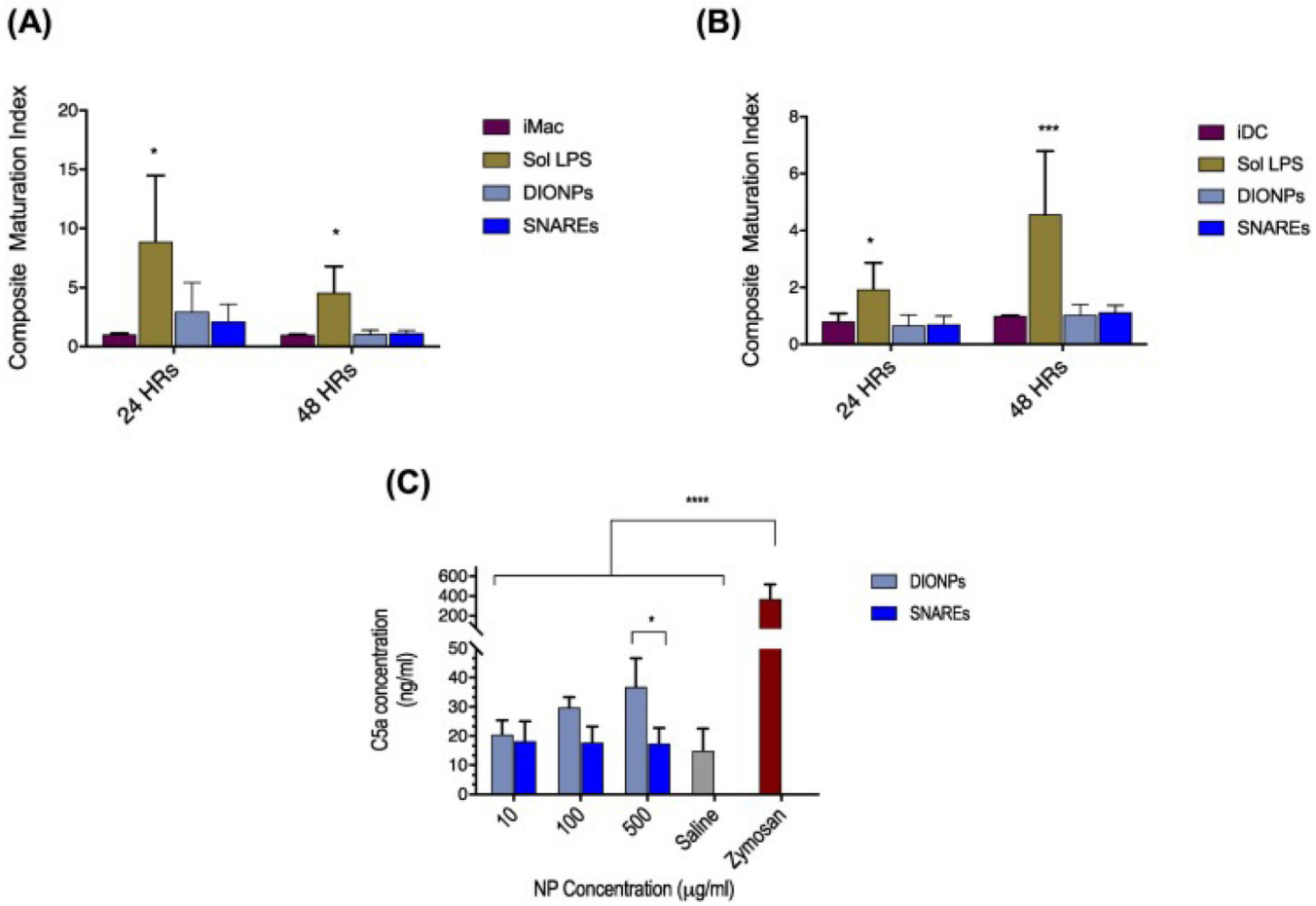

Figure 5.

In vitro assessment of complement activation–C5a generation and phenotypic analysis of dendritic cells and macrophages. **(A)** Bone marrow-derived macrophages demonstrated no significant change in maturation when treated with SNAREs or DIONPs, compared to immature macrophages. (**B)** Bone-marrow-derived DC maturation is unaffected by the presence of DIONPS or SNAREs. (**C)** C5a complement fragment concentration in serum of C57BL/6j mice incubated with DIONPs, SNAREs, saline control, and zymosan positive control for 4 h at 37 °C.

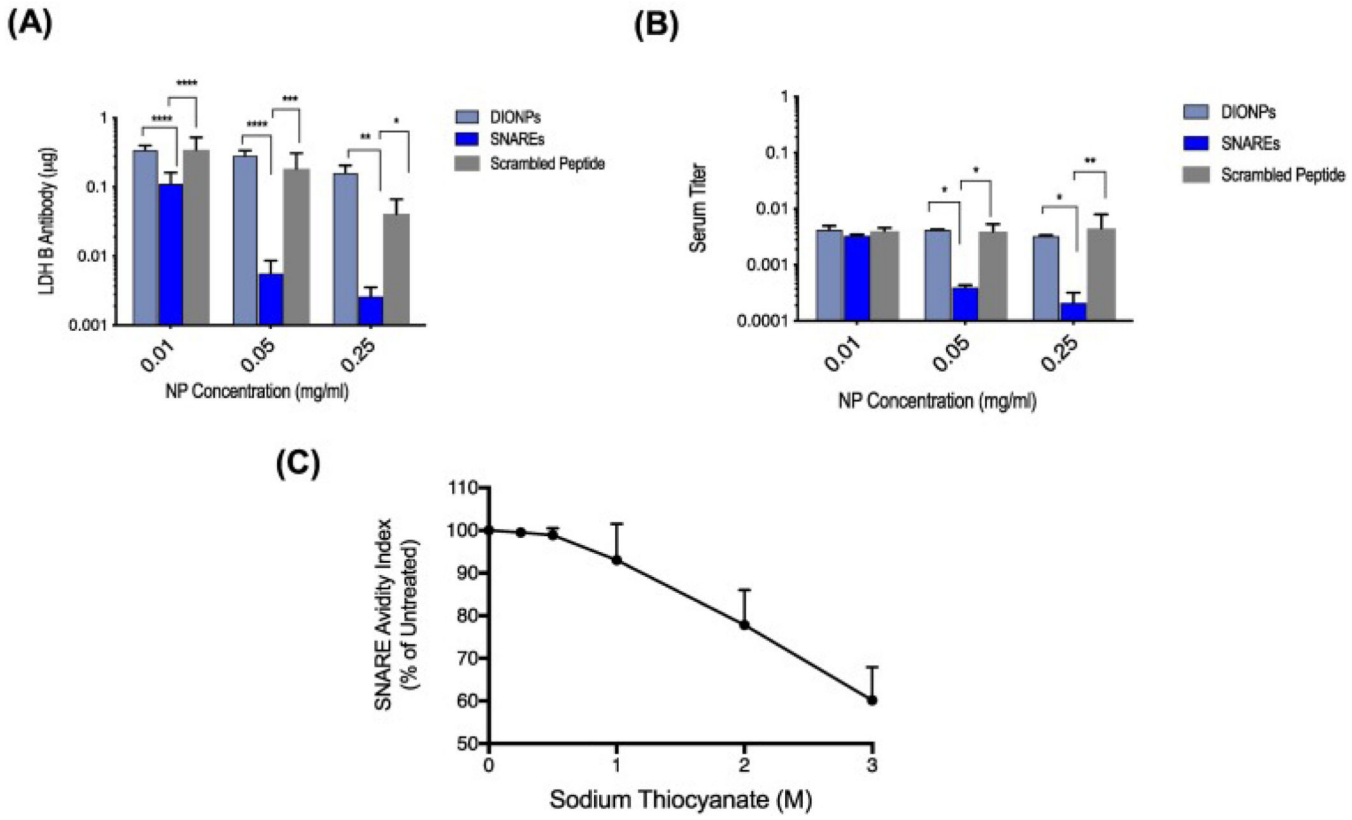

Figure 6.

Assessment of MAR autoantibody capture, specificity, and affinity *in vitro.* **(A)** SNAREs captured up to 2.7 µg LDH B Ab/ mg SNAREs (95% efficiency) and exhibited increased antibody entrapment at higher concentrations. **(B)** SNAREs reduced LDH B antibody titer in human serum by as much as 90% (patient-derived serum of mothers of children with ASD). Scrambled peptide-DIONPs and DIONPs were used as negative controls. **(C)** Avidity of SNAREs to MAR LDH B antibody indicating a 50% avidity index at ~3.6 M sodium thiocyanate concentration.

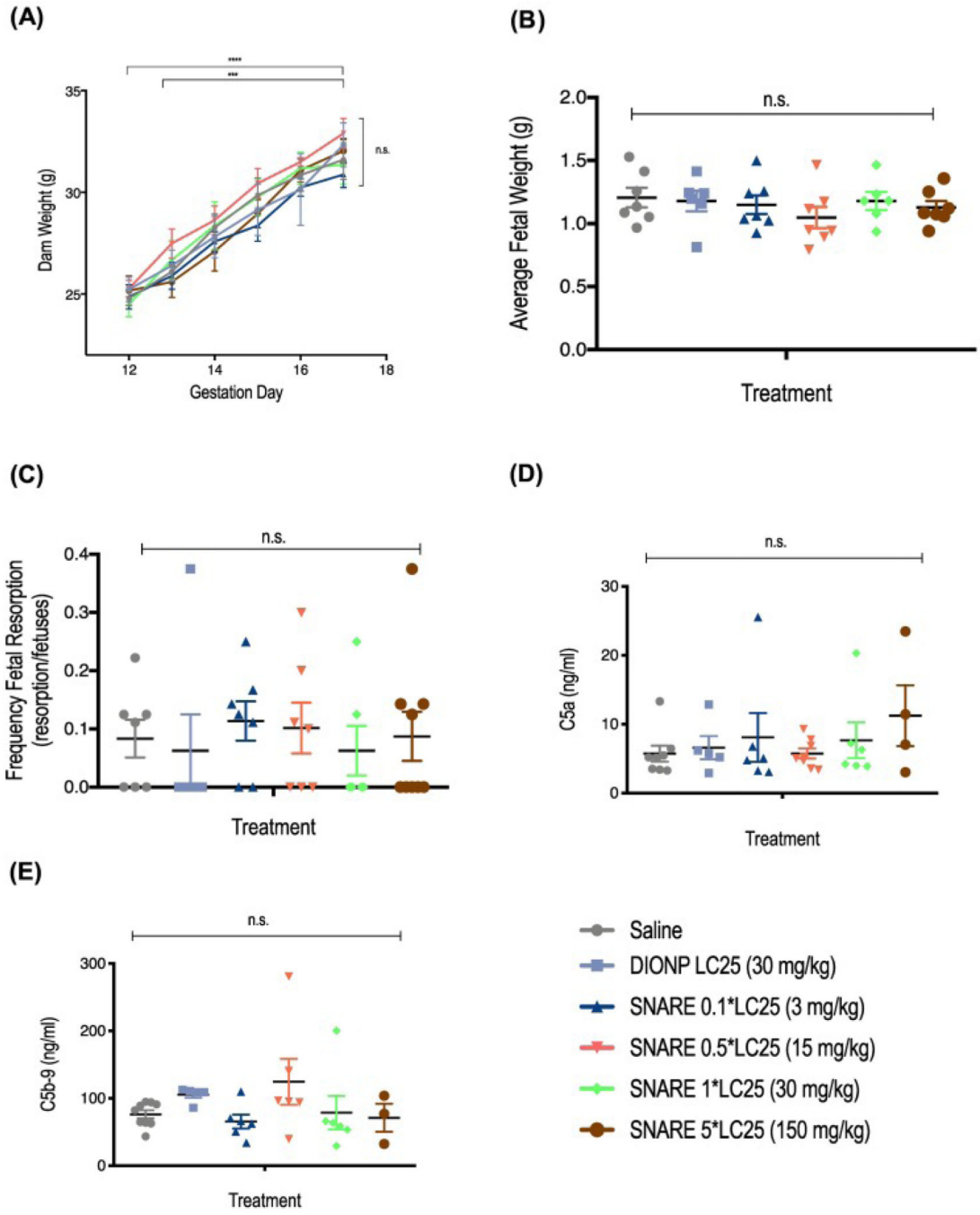

Figure 7.

SNARE maximum tolerated dose (MTD) and assessment of complement activation in pregnant dams. **(A)** Administration of SNAREs did not affect prenatal weight gain. Mice were weighted post-injection from GD 12 to GD 17, when mice were sacrificed for post-mortem analysis. **(B)** Average fetal weight (AFW), determined by dividing the total weight of the uteri by the number of non-resorbed fetuses, is shown. **(C)** Frequency of fetal resorption calculated as number of resorption/number of fetuses of treated compared to saline-treated mice. **(D)** C5a complement factor concentration in serum of mice treated with

SNAREs showed no significant differences to the saline control. **(E)** C5b-9 complement factor concentration in serum of SNARE-treated mice also demonstrated no significant differences compared to saline control.

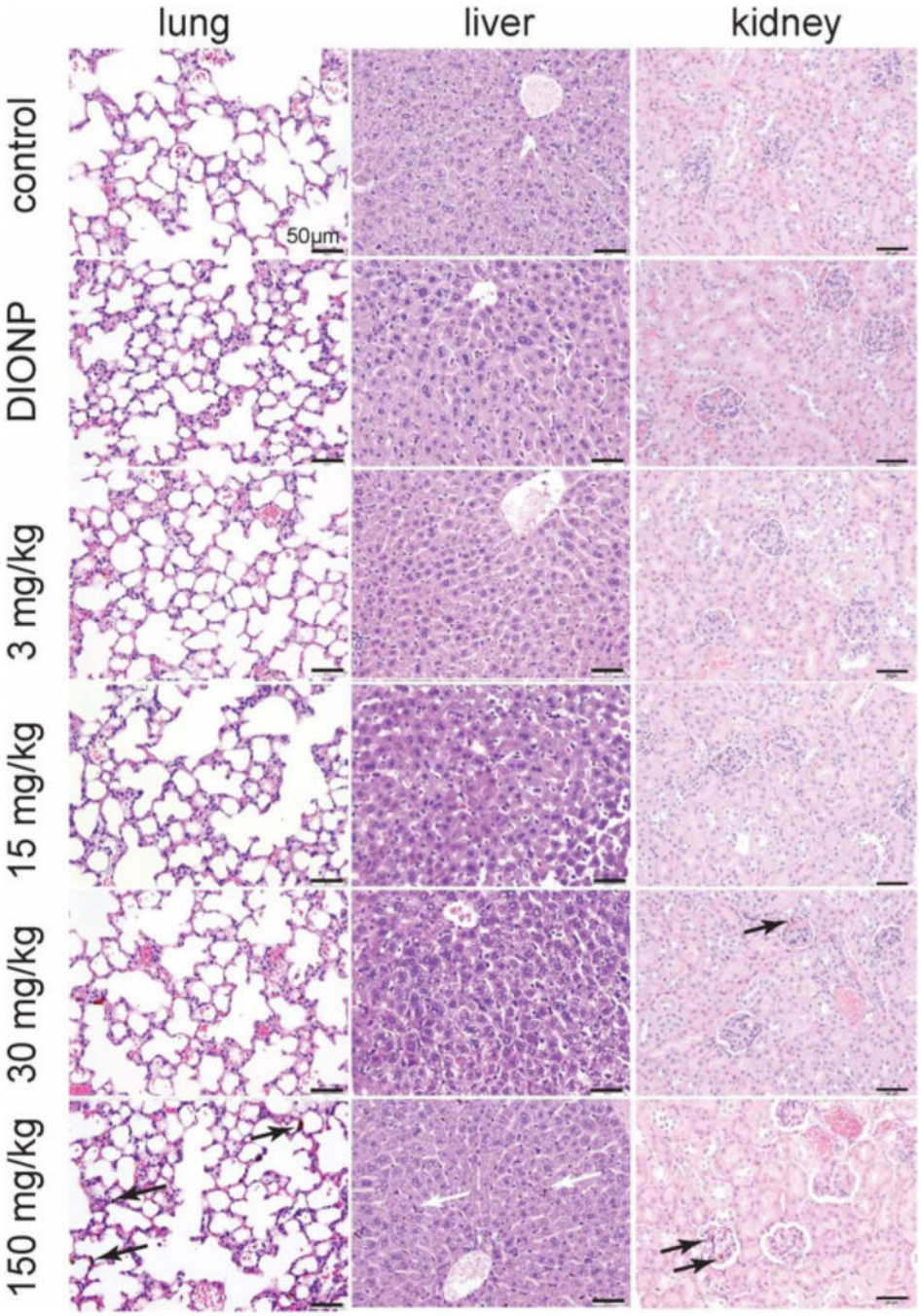

Figure 8.

Histological assessment of SNAREs in lungs, liver, and kidney of pregnant dams. Minimal histological changes were evident in pregnant dams intravenously injected with 3 or 15 mg NPs/kg of SNAREs on GD 12 and sacrificed on GD 17. At 30 mg NPs/kg injection dose of SNAREs and DIONPs, brown pigment (iron deposits) was present in Kupffer cells and rarely within pulmonary capillaries with no evidence of hepatic or lung damage. At the maximal dose of 150 mg/kg, arrows point to high amounts of intravascular iron aggregates observed in the lung sections with mild degree of congestion. In the liver, brown pigment

was observed at moderate to high frequency within Kupffer cells. In the kidney, the brown pigment was present with in glomerular capillaries and occasionally in the renal venules. No evidence of tissue damage or inflammation was associated with the presence of the intravascular deposits in the lung or intracellular pigment in the liver.